

Fed-Listing: Federated Label Distribution Inference in Graph Neural Networks

Suprim Nakarmi

Department of Computer Science
University of Nevada, Las Vegas
Las Vegas, Nevada, USA
nakars2@unlv.nevada.edu

Junggab Son

Department of Computer Science
University of Nevada, Las Vegas
Las Vegas, Nevada, USA
junggab.son@unlv.edu

Yue Zhao

Department of Computer Science
University of Southern California
Los Angeles, California, USA
yue.z@usc.edu

Zuobin Xiong

Department of Computer Science
University of Nevada, Las Vegas
Las Vegas, Nevada, USA
zuobin.xiong@unlv.edu

Abstract—Graph Neural Networks (GNNs) have been intensively studied for their expressive representation and learning performance on graph-structured data, enabling effective modeling of complex relational dependencies among nodes and edges in various domains such as social networks, molecular chemistry, and recommendation systems. However, the standalone GNNs can unleash threat surfaces and privacy implications, as some sensitive graph-structured data is collected and processed in a centralized setting. To solve this issue and achieve data autonomy, Federated Graph Neural Networks (FedGNNs) are proposed to facilitate collaborative learning over decentralized local graph data, aiming to preserve user privacy. Yet, emerging research indicates that even in privacy-preserving settings, shared model updates, particularly gradients, can unintentionally leak sensitive information of local users. Numerous privacy inference attacks have been explored in traditional federated learning and extended to graph settings, but the problem of label distribution inference in FedGNNs remains largely underexplored. In this work, we introduce Fed-Listing (Federated Label Distribution Inference in GNNs), a novel gradient-based attack designed to infer the private label statistics of target clients in FedGNNs without access to raw data or node features. Fed-Listing only leverages the final-layer gradients exchanged during training to uncover statistical patterns that reveal class proportions in a stealthy manner. An auxiliary shadow dataset is used to generate diverse label partitioning strategies, simulating various client distributions, on which the attack model is obtained. Extensive experiments on four benchmark datasets and three GNN architectures show that Fed-Listing significantly outperforms existing baselines, including random guessing and Decaf, even under challenging non-i.i.d. scenarios. Moreover, applying defense mechanisms can barely reduce our attack performance, unless the model’s utility is severely degraded. Our findings expose a critical privacy vulnerability in FedGNNs and highlight the need for more effective defenses against gradient-based information leakage. Our code implementation is available here: <https://github.com/suprimnakarmi/Fed-Listing>.

Index Terms—Federated Learning, Security and Privacy, Graph Neural Networks, Distributed Data Management

I. INTRODUCTION

Graph Neural Networks (GNNs) have emerged as powerful tools for learning from graph-structured data, where both

nodes and edges provide essential information for capturing relational and structural patterns for various tasks. By leveraging message passing and neighborhood aggregation mechanisms, GNNs can capture complex dependencies among nodes in diverse applications such as social networks [1], [2], [3], molecular graphs [4], [5], traffic networks [6], [7], and recommendation systems [8], [9]. However, traditional GNNs training assumes centralized access to the entire graph, which poses significant privacy and scalability challenges when data is distributed across multiple organizations or edge devices.

Federated Graph Neural Networks (FedGNNs) extend the principles of Federated Learning (FL) to graph-based domains, enabling decentralized and privacy-preserving model training without directly sharing raw data [10]. In FedGNNs, individual participants (clients) compute local model updates on their private graph data and only share the model weights or gradients with a central server, which aggregates them to update the global model. This setup is particularly important in privacy-sensitive domains, where data cannot be centralized due to legal, ethical, or security constraints [11], [12], [13]. Real-world use cases include personalized recommendation systems across e-commerce platforms [14], collaborative medical image analysis across hospitals [15], [16], and cross-institutional drug discovery research [17].

Despite its promise, FedGNNs inherit common problems of FL mechanisms and introduce unique challenges due to the interplay between different graph topologies. First, recent studies have shown that even when only the model parameters are shared in FL, they may still leak sensitive information. These shared parameters often retain latent footprints of the underlying private data and are susceptible to manipulation or inversion attacks that can partially or fully reconstruct the original dataset [18], [19]. Moreover, the heterogeneity in local graphs and non-independent and identically distributed (non-i.i.d.) data distributions makes FedGNNs a critical and active area of research. As a result, FedGNNs, in particular, inherit and amplify these vulnerabilities due to the rich relational

structure encoded in graphs. Different attacks have been identified in the FedGNNs literature, including membership inference attacks, where adversaries determine whether a particular data point was part of the training set [20], [21]; property inference attacks, which aim to infer global attributes or properties of the client’s private dataset [22]; graph reconstruction attacks, where attackers attempt to reconstruct nodes, edges, or entire graphs based on shared information [23]; and adversarial attacks that manipulate model updates to degrade global performance or mislead predictions [24]. These attack vectors are well-documented and reflect the importance and growing demand of FedGNN studies. Therefore, understanding the security and privacy implications of federated training on graph data is essential for ensuring robust deployment in sensitive real-world systems.

In this work, we investigate an emerging privacy attack in federated graph neural networks – the Label Distribution Inference (LDI) attack, which has been discussed in a centralized scenario, yet remains underexplored in the FedGNNs settings. Building upon these insights, this paper introduces a practical threat model where the federated server aims to infer the underlying label distribution of a target client, i.e., deducing the statistical distribution of class labels in the target client’s private dataset. To the best of our knowledge, despite the pressing concerns on privacy leakage and downstream model manipulation, the LDI in FedGNNs models is still an open question.

LDI aims to uncover the proportion of each class within a client’s dataset rather than just the presence or absence of specific labels. This exposes highly sensitive information, for instance, estimating the number of patients with tumor-positive versus normal scans in a hospital, or identifying dominant and minority product lines in a retailer’s sales data. Such information can give adversaries an indirect understanding of client data, with a significant impact on privacy and competitive confidentiality for further preference attack and even user profiling.

To launch an effective LDI attack, Fed-Listing is proposed in the horizontal FedGNNs. Fed-Listing leverages an auxiliary dataset for multiple shadow federated training processes under diverse client distribution strategies. From these shadow trainings, we construct an attack dataset by recording gradients of the shadow client parameters, which are then used to train a neural network-based attack model. To validate our attack, we evaluate Fed-Listing on four graph datasets and three widely adopted defense strategies. Our results show that while these defenses mitigate leakage to varying degrees, Fed-Listing consistently outperforms baselines, such as random guessing and Decaf [25], particularly in challenging distribution scenarios, including single-class or one-class-dominant distributions.

Our contributions can be summarized as follows:

- 1) We propose Fed-Listing, the first passive and stealth label distribution inference attack specifically for the horizontal FedGNNs setting.
- 2) The designed shadow-training pipeline in Fed-Listing using an auxiliary dataset explores heterogeneous data

distribution and creates diverse attack scenarios.

- 3) Extensive evaluations are conducted on four benchmark graph datasets and three popular GNN architectures, demonstrating the superior attack performance of Fed-Listing.
- 4) We empirically analyze the resilience of Fed-Listing against three widely adopted defense mechanisms, providing insights on the trade-off between privacy and model utility.

The remainder of the paper is organized as follows. We review the related literature and preliminary knowledge in Section II and Section III. After presenting the model framework in Section IV, we design comprehensive experiments and exhibit results in Section V. To fully understand the method, an ablation study is conducted in Section VI. Finally, this paper is concluded in Section VII.

II. RELATED WORKS

Existing literature related to this work can be categorized into two main branches: label inference attacks in FL and label distribution inference attacks.

A. Label Inference Attacks in FL

Several studies focus on identifying the presence of specific class labels in a client’s dataset within the FL system. For instance, Wainakh et al. proposed Label Leakage by Gradient (LLG), which exploits gradients from the last layer in the federated setting to detect whether a particular label exists in a client’s local training data [26]. Similarly, Meng et al. leverages the message passing mechanism of GNN by adding a single infiltrator (or fake) node to the victim node and uses posterior outputs to infer the presence of label [27]. Arazzi et al. performed a label inference attack in Vertical Federated Learning (VFL) by initializing synthetic labels and iteratively updating them, along with a server model approximation, to minimize the difference between adversarial gradients they generated and the real gradients returned by the server [28]. Apart from the exact label inference, a variant attack targets the preference of a client, referred to as the label profiling attack. Zhou et al. was the first to introduce the Profiling Preference Attack (PPA), exploiting per-class gradient sensitivity to infer a user’s dominant and minority classes [29], in which they trained a meta-classifier that predicts client preferences based on gradient sensitivity across classes. Extending this line, Liu et al. proposed Surrogate Geneartion Preference Profiling (SGPP), a graph-based PPA tailored for VFL, which infers class preferences using only a trained extractor combined with a domain adaptation strategy [30].

In summary, existing label inference attacks in FL are simple, but can not reveal enough information about a target client because they have largely overlooked the client’s label distribution, especially in the FedGNNs scenario, leaving a significant vulnerability under-exploited.

B. Label Distribution Inference Attacks

In the Label Distribution Inference (LDI) attack, the adversary aims to reconstruct the complete label distribution of a client's training dataset. Dai et al. introduced Decaf, which leverages gradient-change magnitudes in the final linear layer to estimate class proportions [25]. Their method first identifies null classes and then fits the proportions of remaining classes using regression against auxiliary per-class gradient bases. Similarly, Gu et al. demonstrated that per-class sample proportions leave distinct traces on output-layer updates [31]. Based on this practice, their approach trains shadow models locally and uses the resulting data to train a CNN-based attack model, which maps sequences of output-layer updates to a client's underlying label distribution. Additionally, Ramakrishna et al. designed four practical estimators that transform a client's last-layer update into an estimate of its label distribution, either through a bias term in the final layer or by using an auxiliary dataset [32]. However, *the above methods are only tested on image datasets, which possess a very different structure and data structures from the graph domain*. Recently, a concurrent work from Cheng et al. proposed EC-LDA, which clips the global model's parameter norm before distributing it to clients, generates Gaussian-sampled dummy data, and collects embedding summaries with softmax outputs [33]. By combining clipped-model gradients with dummy-data statistics, the attacker reconstructs label counts, reverting to the original model afterward to avoid training degradation.

To date, EC-LDA is the only existing work that implements an LDI attack in the FedGNNs setting. However, it relies on embedding compression, meaning the server clips the parameters of the global model to minimize the gradient variance before broadcasting it to the clients. This method assumes an over-realistic threat model, where the server (attacker) can actively tamper with the client model parameters during the training process. Therefore, though the EC-LDA approach assists in the success of the attack, active modification of the training process makes the attack more detectable and potentially disrupts model utility, which is classified as an active attacker. In contrast, our Fed-Listing resides in a passive attacker setting, where the honest-but-curious server only leverages an auxiliary dataset and the attack is undetectable.

III. PRELIMINARY

A. Graph Neural Networks

GNN models are neural network-based models designed to efficiently represent graph-structured data. A graph data is denoted as $G = (V, E, X)$, where V is the set of N nodes, E is the set of edges, and $X \in \mathbb{R}^{N \times d}$ represents the d -dimensional node feature matrix. The edges are represented by an adjacency matrix A of the graph denoted by $A \in \mathbb{R}^{N \times N}$, where $A_{ij} = 1$, if there exists an edge between nodes i and j , and 0 otherwise.

The fundamental principle of GNNs is message passing from the neighboring nodes, where each node iteratively

aggregates information from its neighbors to update its representation. For a node v , the representation at the l^{th} layer is given by:

$$h_v^{(\ell)} = \sigma \left(W^{(\ell)} \cdot \text{AGG} \left(\{h_u^{(\ell-1)} : u \in \mathcal{N}(v)\} \cup \{h_v^{(\ell-1)}\} \right) \right),$$

where $h_v^{(\ell)}$ denotes the embedding of node v at layer ℓ , $\mathcal{N}(v)$ represents the neighbors of v , $W^{(\ell)}$ is a learnable weight matrix, σ is a nonlinear activation function, and AGG is a permutation-invariant function such as mean, sum, or max. Based on the message-passing and aggregation strategies, GNNs are categorized into different types, such as Graph Convolutional Network (GCN), GraphSage, and Graph Attention Network (GAT) [34].

B. Federated Graph Neural Networks

A FedGNNs system integrates FL with GNNs. The server initializes and distributes a global GNN model to all clients. Each client holds its own subgraph $G_i = (V_i, E_i, X_i)$ with private node labels, and trains a local GNN model on this subgraph. The client then returns its model parameters to the server, which aggregates them using weighted aggregation, e.g., FedAvg [35], expressed as:

$$W^{(t)} = \frac{1}{\sum_{j=1}^N a_j} \sum_{i=1}^N a_i W_i^{(t)}, \quad (1)$$

where $W_i^{(t)}$ denotes the local parameters from client i after round t , a_i reflects the relative contribution of client i (e.g., based on data size), and $W^{(t)}$ is the resulting global model. The learning task in FedGNNs can be formulated as the following optimization objective:

$$W = \arg \min_W \sum_{i=1}^N a_i \mathcal{L}(W; G_i, Y_i), \quad (2)$$

where $\mathcal{L}(\cdot)$ is the task-specific loss function, and Y_i denotes the labels on nodes or edges within client's subgraph G_i .

FedGNNs are further categorized into two categories: Horizontal FedGNNs and Vertical FedGNNs. In the Horizontal FedGNNs, clients share graphs with the same feature and label space but different node sets, while in the vertical setting, clients possess graphs that share the same node set but contain different feature spaces or edge relations. The proposed method in this paper is specifically for horizontal FedGNNs.

IV. METHODOLOGY: FED-LISTING

In this section, we first discuss the problem setting of the targeted FedGNNs scenario and then detail the attack method and algorithms.

A. Problem Formulation

Consider the horizontal FedGNNs scenario with a set of M clients: $S = \{S_1, \dots, S_M\}$, where each client S_k holds a local graph: $G^{(k)} = (A^{(k)}, X^{(k)})$, with $A^{(k)} \in \mathbb{R}^{N_k \times N_k}$ representing adjacency matrix of edges on N_k nodes and

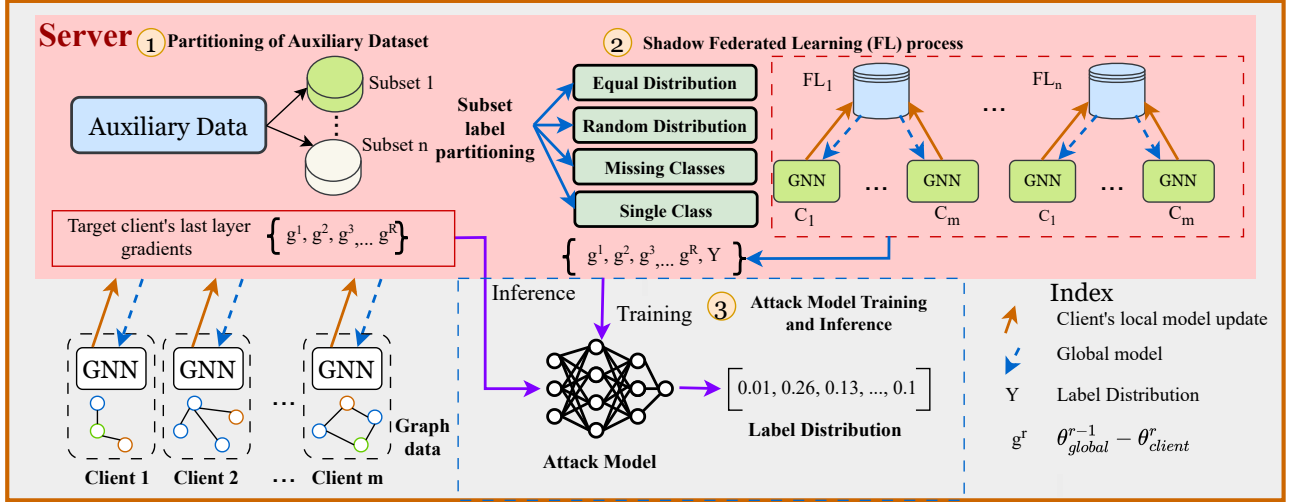


Fig. 1: Overview of the proposed attack: Fed-Listing. All clients train an identical GNN (chosen from three variants) to train on one of four graph datasets. Each auxiliary data subset is further partitioned based on four criteria: single class, random distribution, equal distribution, and missing classes. Multiple independent shadow training sessions in the FL setting are performed to generate attack data.

$X^{(k)} \in \mathbb{R}^{N_k \times d}$ is the node-feature matrix in a shared d -dimensional space. During the FL training process, all labels of a client S_k , denoted as $\mathbf{y}^{(k)} \in \{1, \dots, T\}^{N_k}$, remain on the clients as privacy information. The goal of the attacker is to infer the label distribution in the victim client, i.e., per-class proportions.

In FedGNN, a global graph model (e.g., GCN, depending on the system configuration) $h(\cdot; \theta): (A, X) \mapsto \hat{Y} \in \mathbb{R}^{N \times T}$ is initialized at the server with parameter θ . At communication round t , the server broadcasts the aggregated model from the last round, θ^{t-1} , to every participating client in the FL system. Each client S_k then performs E local epochs of the local training algorithm on its local private data following Eq. (3):

$$\theta_k^t = \theta^{t-1} - \eta \nabla_{\theta} \left[\frac{1}{N_k} \sum_{u=1}^{N_k} \ell(h(A^{(k)}, X^{(k)})_u; y_u^{(k)}) \right], \quad (3)$$

where ℓ is the per-node cross-entropy loss and $h(\cdot)_u$ denotes the output (logits) at node u . Once local updates are complete, each client sends θ_k^t back to the server, which aggregates them via weighted averaging, e.g., Federated Averaging (FedAvg) [35], $\theta^t = \sum_{k=1}^M \frac{N_k}{\sum_{j=1}^M N_j} \theta_k^t$. Equivalently, horizontal FL on graph data seeks to solve the global objective as follows,

$$\theta^* = \arg \min_{\theta} \sum_{k=1}^M \frac{N_k}{\sum_{j=1}^M N_j} \mathbb{E}_{u \sim U_k} [\ell(h(A^{(k)}, X^{(k)})_u; y_u^{(k)})]. \quad (4)$$

The FedAvg procedure integrates these local optimization steps with server-side aggregation, enabling the shared GNN parameters to reflect patterns across all sets of disjoint nodes, without exchanging raw adjacency or feature data. Formally, the attacker in this setting aims to infer the label distribution

of the target client S_k as denoted by $\{y_1^{(k)}, y_2^{(k)}, \dots, y_T^{(k)}\}$, where $y_t^{(k)}$ denotes proportion of class c and $\sum_{t=1}^T y_t^{(k)} = 1$.

B. Threat Model

In our attack setting, the FL server acts as an honest-but-curious adversary, attempting to infer the label distribution of a target client's training data. While the FL process itself remains unaffected, the server can exploit the last layer gradients of the target client on each FL round to carry out the inference.

Adversary's knowledge: As the server serves as the attacker, it has full access to the parameters shared by the clients and the label space of the training dataset. Also, the server has access to an auxiliary dataset, which consists of a similar distribution and label space as the real dataset of FL clients.

Adversary's capability: The adversary can leverage the model parameters received from each client across each round to extract information and deduce the underlying label distribution of the target client's local data.

C. Fed-Listing Schema

In this section, we provide a detailed description of the proposed Fed-Listing method. The attack proceeds in three main phases: (1) partitioning of the auxiliary dataset, (2) shadow FL training process, and (3) attack model training and inference as shown in Figure 1.

1) Partitioning of the Auxiliary Dataset: The auxiliary dataset \mathcal{D}_a was first divided into n subsets, each containing approximately equal proportions of samples across all classes. Each subset was further partitioned into multiple clients to simulate FL participants. To capture diverse local data distributions, we design four partitioning strategies (or scenarios): (i) Equal proportion: all classes are equally represented in each client, (ii) Random distribution: classes are assigned randomly

across clients, (iii) Single-class: each client is assigned samples from only one class, (iv) Missing classes: some classes are absent from certain clients. These partitions were selected to cover the scenarios that are i.i.d. and non-i.i.d. in FL [36].

For each partition category, an independent FL process was conducted to ensure that local data heterogeneity was fully represented. Since auxiliary datasets are typically limited in size, resampling techniques across different partitioning categories were permitted. However, within any given FL scenario, the data assigned to each client remained independent to preserve the integrity of the local distributions. For each scenario, we empirically report the number of FL process and the number of clients with a given (non-i.i.d.) label distribution required for the attack to succeed, and the results are shown in Figure 3. For example, in the *Random distribution* setting, we illustrate (Figure 3(a)) that the attack performed better as we increased the number of FL processes. Similarly, for *Single-class* and *Missing-class* settings, we show that the FL process with clients having more proportion of each case yielded higher attack performance.

2) *Shadow FL Training Processes*: During federated training, in each communication round r , the gradients of the last layer are collected from all participating clients. Specifically, the gradient update for round r is defined as follows,

$$g^r = \theta_{\text{global}}^{r-1} - \theta_{\text{client}}^r, \in \mathbb{R}^{d_{\text{out}}}, \quad (5)$$

where $\theta_{\text{global}}^{r-1}$ is the global model distributed at the beginning of round r , θ_{client}^r is the locally updated model parameter after round r , and d_{out} is the output dimension. Over R communication rounds, the complete gradient record for a client k is represented as,

$$G_k = [g_k^1, g_k^2, \dots, g_k^R] \in \mathbb{R}^{R \times d_{\text{out}}},$$

For example, if there are C clients and R communication rounds, the server can obtain C feature vectors of size R each. For each data partitioning setting, we collected the last-layer gradients from individual clients, yielding a set of gradient records $\{G_k\}_{k=1}^i$, where i denotes the number of clients. Each client's gradients have their corresponding label distribution, which serves as the ground-truth target for training. To construct the attack dataset, the gradients from all clients are concatenated and flattened into fixed-length feature vectors to ensure compatibility with the neural network-based attack model. Exploiting the parameters or gradients of the final layer is a popular approach for inferring training data, specifically for recovering labels and label distributions, as demonstrated in several prior works [31], [25], [37].

3) *Attack Model Training and Inference*: The recorded gradients, paired with their corresponding label distributions, form the training dataset for the attack model. Formally, each training sample is represented as (G_k, Y) , where $Y = \{y_1, y_2, \dots, y_T\}$ is the ground truth label distribution of the client, with $\sum_{i=1}^T y_i = 1$. Then, a neural network-based attack model is trained to infer label distributions of clients. The objective is to minimize the discrepancy between the predicted

Algorithm 1 Fed-Listing Algorithm

Input: Auxiliary dataset \mathcal{D}_a , clients C , rounds R , local epochs E , partition strategies \mathcal{P} , loss weights (a, b, c)
Output: Trained attack model $\hat{\mathcal{A}}$
Split \mathcal{D}_a into subsets $\{\mathcal{D}_a^{(1)}, \dots, \mathcal{D}_a^{(n_s)}\}$

- 1: **for** each subset $\mathcal{D}_a^{(s)}$ and strategy $p \in \mathcal{P}$ **do**
- 2: Partition $\mathcal{D}_a^{(s)}$ into C clients
- 3: **for** $r = 1$ to R **do**
- 4: **for** each client k **do**
- 5: Train locally for E epochs
- 6: Record last-layer update $g_k^r = \theta_{\text{global, last layer}}^{r-1} - \theta_{k, \text{last layer}}^r$
- 7: **end for**
- 8: Aggregate updates $\rightarrow \theta_{\text{global}}^r$
- 9: **end for**
- 10: **for** each client k **do**
- 11: $G_k \leftarrow [g_k^1, \dots, g_k^R]$, flatten to G_k^{flat}
- 12: $Y_k \leftarrow$ label distribution of D_k
- 13: Add (G_k^{flat}, Y_k) to attack dataset $\mathcal{T}_{\text{attack}}$
- 14: **end for**
- 15: **end for**
- 16: Train attack model \mathcal{A} on $\mathcal{T}_{\text{attack}}$ with loss
- 17: **return** trained attack model $\hat{\mathcal{A}}$

label distribution \hat{Y} and the ground truth Y . To achieve this, we employ a composite loss function that combines multiple distribution-similarity measures:

$$\mathcal{L}(Y, \hat{Y}) = aL_{L1}(Y, \hat{Y}) + bL_{\text{Var}_L}(Y, \hat{Y}) + cL_{JS}(Y, \hat{Y}), \quad (6)$$

where

$$L_{L1}(Y, \hat{Y}) = \frac{1}{T} \sum_{t=1}^T |y_t - \hat{y}_t|, \quad (7)$$

$$L_{\text{Var}_L}(Y, \hat{Y}) = \left(\text{Var}(Y) - \text{Var}(\hat{Y}) \right)^2, \quad (8)$$

$$L_{JS}(Y \parallel \hat{Y}) = \frac{1}{2} \text{KL}(Y \parallel M) + \frac{1}{2} \text{KL}(\hat{Y} \parallel M), \quad (9)$$

where $M = \frac{1}{2}(Y + \hat{Y})$, and $\text{KL}(\cdot \parallel \cdot)$ is the Kullback-Leibler divergence between two probability distributions, y_t denotes the ground truth labels, \hat{y}_t is the predicted label, T is the total number of class. The parameters a, b , and c are scalar weights balancing the contribution of each term. To select the optimum combination of loss function, we listed the types of alignment and distribution matching (or overlapping) loss functions used for distribution learning [38], [39], [40]. The alignment loss (e.g., L1 norm) compares individual elements in two distributions and is generally used to measure the statistical discrepancy between two or more data distributions. In contrast, distribution matching loss (e.g., JS-divergence and KL) addresses the degree of overlap or separation between the distinct distributions. We empirically selected the objective

TABLE I: Description of datasets including the number of nodes, edges, features, and label classes on each dataset.

Dataset	Nodes	Edges	Features	Classes
Cora	2,708	5,429	1,433	7
PubMed	19,717	44,338	500	3
Citeseer	3,327	4,732	3,703	6
Amazon Computers	13,752	245,861	767	10

function(s) that yielded the best performance as shown in Table V and fixed the loss function form in Eq. (6).

The optimum values for hyperparameters a , b , and c were selected using grid search on values from 0 to 1 with a step size of 0.25. The combinations that resulted in the lowest loss were selected as optimum values. For the Cora and Citeseer dataset, the best performance was observed when a , b , and c were set to 0.0, 0.5, and 0.5, whereas PubMed and Amazon Computer had the best result when the values of a , b , and c were set to 0.5, 0.25, and 0.25.

V. EXPERIMENT RESULTS

In this section, we simulate the proposed attack method Fed-Listing on real-life datasets, compare it with the existing attack baselines, and evaluate the attack robustness against popular defense mechanisms.

A. Experiment Settings

Datasets. To evaluate the effectiveness of Fed-Listing, we conducted experiments on four widely used graph benchmarks: Cora [41], PubMed [41], Citeseer [41], and Amazon Computers [42], under varying client label distributions. These datasets are chosen to assess the accuracy of our proposed attack in recovering each client’s label distribution. Cora, PubMed, and Citeseer are citation network datasets, where the nodes correspond to scientific papers and the edges represent citation links. In Cora and Citeseer, each paper is encoded using a Bag-of-Words (BoW) feature vector, while in PubMed, features are represented using Term Frequency–Inverse Document Frequency (TF-IDF) weighted word vectors. Amazon Computers is a co-purchase network, where the nodes represent products in the “Computers” category and the edges denote co-purchase relationships – such as laptops purchased alongside covers or mice. Product features in this dataset are also represented using BoW vectors derived from metadata, e.g., product descriptions and reviews. A detailed summary of the datasets and their properties is provided in Table I.

GNN Architecture and Baselines. We evaluate our method using three widely adopted GNN architectures: GCN [43], GraphSage [44], and Graph Isomorphism Network (GIN) [45]. While all these models follow the fundamental message-passing paradigm, where node representations are updated by aggregating information from neighboring nodes, they differ primarily in their aggregation strategies. GCN generalizes convolution operations to graphs by applying a linear transformation to node features aggregated via a normalized adjacency matrix. GraphSage improves scalability by sampling a fixed-size set of neighbors and aggregating their features using a

learnable function. GIN, recognized for its expressive power, employs a sum aggregator followed by an MLP, allowing it to capture complex graph structures with high fidelity.

To assess the effectiveness of our Fed-Listing attack, we compare it against three baselines. The first one is random guessing, which estimates the label distribution of each target client by sampling from a normal distribution, providing a minimal performance reference. The second baseline is Decaf [25], a recent method designed for label distribution inference attack in FL, but on image data. We configure the source code to make it fit the graph data input as a passive attacker baseline. We include Decaf as it shares a similar threat model and evaluation setting, particularly in scenarios where clients exhibit uniform or skewed label distributions, making it a strong and relevant baseline for comparison. The third baseline is EC-LDA [33], which is designed as an active attacker by manipulating the training parameters and FL process. Though the active attacker has the limitation of being detected, it can serve as a practical upper bound, justifying the performance of our passive attack methods.

Evaluation Metrics. Since the attacker infers the proportion of each label, we compare the alignment of the inferred distribution $Y = (y_1, \dots, y_T)$ and the ground truth label distribution $\hat{Y} = (\hat{y}_1, \dots, \hat{y}_T)$. For consistency in previous works [33], [31], we selected three evaluation metrics: Manhattan Distance (MD), JS-divergence, and Cosine Similarity (CS). $MD(Y, \hat{Y}) = \sum_{t=1}^T |y_t - \hat{y}_t|$ measures the difference between each of the classes to provide a total deviation measure between two distributions. JS-divergence, illustrated in Eq. (9), is symmetric and bounded between 0 and 1, making it a stable metric to measure the distributional divergence. In contrast, CS measures the directional similarity of the two distributions and shows how well the predicted and true distributions align in the same direction, $CS(Y, \hat{Y}) = \frac{\sum_{t=1}^T y_t \hat{y}_t}{\sqrt{\sum_{t=1}^T y_t^2} \sqrt{\sum_{t=1}^T \hat{y}_t^2}}$. For MD and JS-divergence, smaller values indicate a better match to the ground truth distribution. Whereas higher values of the CS suggest stronger alignment with the ground truth.

Attack Scenarios. An auxiliary dataset typically consists of samples drawn from a similar (or a closely related) distribution as the target client’s private training data and is employed to train shadow models for performing attacks. We partition each dataset \mathcal{D} into two **disjoint** subsets: the training set \mathcal{D}_T and the auxiliary set \mathcal{D}_a . In this partitioning, we reserve 20% of the original data as \mathcal{D}_a for our attack to succeed. To evaluate the effectiveness of the attack, we considered five scenarios with varying class distribution proportions, as summarized in Table II, III, IV. In the Equal proportion setting, each class was represented equally, whereas in the Random split scenario, class proportions were assigned randomly. In the One-class-missing case, a randomly chosen class was absent. The Single-class-only scenario includes samples from just one class, while the one-class-dominant case features one class with the highest proportion compared to the others. To further examine the robustness of our attack, we also evaluate its performance under three popular defense strategies: Differential Privacy

(DP), noisy gradients, and gradient compression.

Implementation Details. We implemented Fed-Listing using the Flower FL framework (v1.19.0), with integration of PyTorch (v2.7.1) and PyTorch Geometric (v2.6.1) for GNN training. Each experiment employed a consistent two-layer GNN architecture across all clients to ensure comparability. We used $C = 10$ clients and conducted $R = 50$ communication rounds. For local training, each client applied the Adam optimizer with a learning rate of 0.001 and a batch size of 32. To support the attack, we recorded the gradients of the final GNN layer from each client at the end of every communication round. These gradients were then transformed into structured feature vectors, serving as inputs to our attack model.

The attack model was designed as a Multi-Layer Perceptron (MLP) with two hidden layers containing 256 and 128 units, respectively, and ReLU activations. The training was performed on last-layer gradients obtained from shadow datasets created via four different client partitioning strategies: single-class, random distribution, equal distribution, and missing-class configurations. In experiments with limited auxiliary data, we allowed repeated use of samples across different partitioning strategies while ensuring that each client's data remained independent within a given federated setting. The attack model was optimized using a composite loss function as defined in Eq. (6).

B. Attack Performance and Analysis

The results in Table II, Table III, and Table IV illustrate the effectiveness of Fed-Listing across all datasets and partitioning strategies when using GCN, SAGE, and GIN as a local client model, respectively. For example, in Table II on GCN models, our attack method generally achieves the lowest MD and JS-divergence, as well as the highest cosine similarity, compared to both random guessing and Decaf. Specifically, under the equal proportion setting, our Fed-Listing performs nearly perfectly, with JS-divergence as 0.000 and CS exceeding 0.985 on the Citeseer dataset. Non-i.i.d. scenarios highlight the clear superiority of our approach against the two baselines (Random and Decaf) in GCN. For example, in the challenging One-class missing and One-class dominant scenario, where clients hold highly skewed data distribution, our Fed-Listing maintains best performance (e.g., Cosine Similarity of 0.971 and JS divergence of 0.002 on the Cora dataset), while Decaf and random guessing show a significant decline. Similar performance of our Fed-Listing method can be observed on GraphSage and GIN models. However, for non-i.i.d. cases, the performance gap is narrow, and Decaf sometimes overtakes on specific metrics. Notably, Decaf exhibits moderate success in some balanced settings but struggles significantly in highly skewed distributions, particularly evident on Amazon Computers, where its CS drops drastically.

Remark. The performance of EC-LDA is displayed for reference in the tables. As expected, the active attack EC-LDA, due to its stronger attack assumption that purposely manipulates the model parameters during FL training, allows the malicious server to deceive the local client into revealing

more information in the next training round. Therefore, the EC-LDA attack can achieve a nearly perfect LDI attack result, yet it comes with the vulnerability of easy detection and the cost of training accuracy for GNN tasks.

Generally, across all methods on the majority of experiments, we observe that the label distribution inference is easier in the Equal and Random split settings, but more challenging in the Single class only and One-class dominant scenarios. This difficulty likely arises because the gradients in these cases were dominated by the majority of clients having more balanced class proportions.

C. Attack Robustness against Defense Strategy

In this section, we evaluate the robustness of Fed-Listing under three widely adopted defense strategies: DP [46], [47], noisy gradients [48], and gradient compression [49]. DP ensures that the influence of any single training example on the shared model update is bounded, typically enforced through the (ϵ, δ) -DP, where ϵ controls privacy loss and δ denotes the probability of failure. Using the Gaussian mechanism, noise with standard deviation $\sigma = \sqrt{2 \ln(1.25/\delta)}$ is added to clipped gradients, balancing privacy and utility. The noisy gradient defense applies noisy perturbation directly to client gradients in each communication round, with the update $\tilde{g} = g + \mathcal{N}(0, \sigma^2 I)$, where g denotes the original gradient and σ scales the injected noise. This additional noise reduces information leakage while maintaining training feasibility. Lastly, gradient compression reduces the communication footprint and obscures fine-grained information by transmitting only the significant gradient elements with the largest magnitudes, defined as $\tilde{g}_i = g_i$ if $|g_i| \geq \tau$, and $\tilde{g}_i = 0$ otherwise, where τ is the threshold chosen such that only a fraction α of gradients are preserved. Together, these defenses aim to diminish the attack surface of inference attacks in federated learning.

Figure 2 compares the impact of DP, noisy gradients, and gradient compression on the attack robustness of Fed-Listing (in terms of JS-divergence). Under the DP defense, the performance of FedGNNs improves as the privacy budget ϵ increases. However, this comes at the cost of privacy: the attack becomes significantly more effective at that point when the privacy budget ϵ increases, except when ϵ equals 2 and 3, where the attack performance was reduced. In the case of noisy gradients, increasing the noise level leads to a steep decline in model accuracy - from 0.701 at $\sigma = 0.5$ to just 0.473 at $\sigma = 3$. Meanwhile, attack effectiveness remains moderate at intermediate noise levels but deteriorates further at higher noise scales (e.g., $\sigma \geq 2.5$), where both model utility and attack reliability break down. In contrast, gradient compression demonstrates a more favorable trade-off. Accuracy steadily improves with higher compression ratios – from 0.547 at $\alpha = 0.1$ to 0.725 at $\alpha = 1.0$, while attack success is notably minimized around $\alpha = 0.5$ (JS-divergence = 0.118).

In summary, it is hard for these three defense mechanisms to mitigate the proposed Fed-Listing attack with slight defense strength, and a stronger defense strength (e.g., larger noise scales) can cause much utility loss.

TABLE II: Performance under different client-data splits and distance/divergence measures. All reported metrics were obtained using the GCN model in both FL training and shadow FL training. AC: Amazon Computers. The highest performance is denoted in bold text.

Datasets	Target label distribution	Manhattan distance (↓)				Jensen-Shannon divergence (↓)				Cosine similarity (↑)			
		ours	Random	Decaf	EC-LDA	ours	Random	Decaf	EC-LDA	ours	Random	Decaf	EC-LDA
Cora	Equal proportion	0.221	0.399	0.422	0.000	0.001	0.003	0.004	0.000	0.973	0.918	0.871	1.000
	Random split	0.183	0.471	0.796	0.012	0.002	0.007	0.025	0.000	0.971	0.888	0.547	0.999
	One class missing	0.183	0.471	0.635	0.006	0.002	0.007	0.119	0.005	0.971	0.888	0.762	1.000
	Single class only	1.287	1.787	1.350	0.000	0.035	0.053	0.375	0.000	0.778	0.223	0.734	1.000
	One-class dominant	1.095	0.968	1.335	0.000	0.029	0.033	0.062	0.000	0.704	0.766	0.399	1.000
PubMed	Equal proportion	0.166	0.315	0.336	0.000	0.001	0.005	0.006	0.000	0.982	0.948	0.941	1.000
	Random split	0.093	0.582	0.812	0.012	0.000	0.017	0.559	0.000	0.994	0.821	0.698	0.999
	One class missing	0.243	0.382	0.353	0.059	0.003	0.007	0.008	0.010	0.968	0.918	0.913	0.999
	Single class only	1.196	0.940	1.000	0.000	0.081	0.620	0.370	0.000	0.683	0.842	0.520	1.000
	One-class dominant	0.783	1.583	0.708	0.013	0.030	0.275	0.037	0.000	0.812	0.188	0.795	1.000
Citeseer	Equal proportion	0.152	0.334	0.147	0.000	0.000	0.002	0.001	0.000	0.985	0.943	0.980	1.000
	Random split	0.107	0.336	0.244	0.008	0.000	0.004	0.002	0.000	0.993	0.918	0.956	0.999
	One class missing	0.412	0.625	0.692	0.017	0.011	0.115	0.115	0.002	0.902	0.800	0.783	0.999
	Single class only	1.676	1.615	1.292	0.003	0.568	0.544	0.050	0.000	0.391	0.450	0.469	1.000
	One-class dominant	0.928	1.467	1.217	0.029	0.039	0.082	0.042	0.002	0.559	0.304	0.710	0.999
AC	Equal proportion	0.435	0.489	0.706	0.000	0.003	0.004	0.084	0.000	0.903	0.852	0.746	1.000
	Random split	0.225	1.050	0.953	0.089	0.001	0.023	0.016	0.002	0.966	0.493	0.564	0.998
	One class missing	0.617	0.805	0.665	0.000	0.068	0.034	0.027	0.000	0.858	0.068	0.810	1.000
	Single class only	0.860	1.732	1.874	0.027	0.038	0.351	0.387	0.004	0.771	0.344	0.189	1.000
	One-class dominant	1.415	1.543	1.544	0.081	0.043	0.069	0.063	0.003	0.361	0.069	0.166	0.999

TABLE III: Performance under different client-data splits and distance/divergence measures. All reported metrics were obtained using the GraphSage model in both FL training and shadow FL training. AC: Amazon Computers. The highest performance is denoted in bold text.

Datasets	Target label distribution	Manhattan distance (↓)				Jensen-Shannon divergence (↓)				Cosine similarity (↑)			
		ours	Random	Decaf	EC-LDA	ours	Random	Decaf	EC-LDA	ours	Random	Decaf	EC-LDA
Cora	Equal proportion	0.313	0.399	0.413	0.000	0.003	0.004	0.004	0.000	0.921	0.918	0.918	1.000
	Random split	0.146	0.471	0.796	0.000	0.001	0.007	0.025	0.000	0.985	0.888	0.888	1.000
	One class missing	0.542	0.471	0.288	0.010	0.154	0.119	0.019	0.000	0.743	0.762	0.964	1.000
	Single class only	0.703	1.787	1.350	0.000	0.224	0.536	0.375	0.000	0.889	0.223	0.734	1.000
	One-class dominant	1.053	1.517	1.335	0.000	0.026	0.083	0.062	0.000	0.742	0.201	0.399	1.000
PubMed	Equal proportion	0.237	0.315	0.330	0.000	0.003	0.005	0.006	0.000	0.969	0.948	0.941	1.000
	Random split	0.026	0.582	0.818	0.013	0.000	0.017	0.559	0.000	0.999	0.821	0.698	0.999
	One class missing	0.808	1.583	0.355	0.045	0.031	0.275	0.008	0.000	0.788	0.188	0.913	0.999
	Single class only	0.562	0.940	1.000	0.012	0.358	0.624	0.370	0.002	0.960	0.842	0.520	1.000
	One-class dominant	0.146	0.621	0.708	0.024	0.001	0.019	0.037	0.000	0.996	0.878	0.795	0.999
Citeseer	Equal proportion	0.169	0.334	0.229	0.000	0.002	0.003	0.002	0.000	0.959	0.943	0.980	1.000
	Random split	0.490	0.335	0.222	0.007	0.000	0.007	0.001	0.000	0.998	0.908	0.956	1.000
	One class missing	0.329	0.625	0.692	0.017	0.025	0.111	0.106	0.001	0.946	0.802	0.783	0.999
	Single class only	0.730	1.615	1.922	0.000	0.052	0.544	0.056	0.000	0.889	0.450	0.469	1.000
	One-class dominant	0.900	1.467	1.205	0.001	0.038	0.082	0.042	0.001	0.710	0.304	0.710	1.000
AC	Equal proportion	0.518	0.370	0.706	0.001	0.002	0.002	0.084	0.000	0.841	0.928	0.746	1.000
	Random split	0.155	0.579	0.953	0.072	0.000	0.011	0.016	0.001	0.990	0.776	0.776	0.999
	One class missing	0.242	0.788	0.665	0.002	0.055	0.086	0.027	0.000	0.954	0.695	0.810	1.000
	Single class only	1.834	1.537	1.874	0.035	0.479	0.378	0.387	0.006	0.195	0.583	0.189	1.000
	One-class dominant	1.058	1.155	1.544	0.084	0.021	0.036	0.063	0.004	0.721	0.609	0.609	0.999

VI. ABLATION STUDY

In this section, we discuss the contribution of each stage of the attack method. Specifically, we evaluate the selection of the number of FL processes required to create the Fed-Listing training dataset and the loss function combination, which determines the optimal attack parameters.

A. The Impact of Shadow FL Processes

We empirically determine the number of FL processes required for each partition scenario to perform a success-

ful attack. Additionally, for Partitions 2, 3, and 4, we also determine the impact of attack performance when changing the proportion of clients having the specified partition label distribution. Figure 3 demonstrates ablation results for various FL processes, where cosine similarity was used to measure how closely the attack-inferred label distribution matches the ground truth. Figure 4 illustrates the performance of the attack when the proportion of clients having a specific partition is changed. We evaluate up to 20 shadow FL processes because using more processes increases the probability of

TABLE IV: Performance under different client-data splits and distance/divergence measures. All reported metrics were obtained using the GIN model in both FL training and shadow FL training. AC: Amazon Computers. The highest performance is denoted in bold text.

Datasets	Target label distribution	Manhattan distance (↓)				Jensen-Shannon divergence (↓)				Cosine similarity (↑)			
		ours	Random	Decaf	EC-LDA	ours	Random	Decaf	EC-LDA	ours	Random	Decaf	EC-LDA
Cora	Equal proportion	0.216	0.471	0.422	0.000	0.001	0.008	0.004	0.000	0.973	0.888	0.874	1.000
	Random split	0.117	0.664	0.776	0.010	0.000	0.015	0.025	0.000	0.993	0.711	0.547	0.999
	One class missing	0.654	0.288	0.635	0.001	0.188	0.019	0.119	0.000	0.657	0.964	0.762	1.000
	Single class only	1.687	1.787	1.350	0.000	0.493	0.536	0.375	0.000	0.334	0.223	0.734	1.000
	One-class dominant	0.844	1.517	1.335	0.001	0.016	0.083	0.062	0.000	0.872	0.201	0.399	1.000
PubMed	Equal proportion	0.132	0.315	0.336	0.000	0.000	0.005	0.006	0.000	0.990	0.948	0.941	1.000
	Random split	0.130	0.582	0.812	0.017	0.001	0.018	0.059	0.000	0.990	0.821	0.698	0.999
	One class missing	0.816	1.583	0.353	0.045	0.032	0.275	0.008	0.000	0.781	0.188	0.913	0.999
	Single class only	1.215	0.940	1.000	0.059	0.828	0.624	0.370	0.010	0.662	0.842	0.520	0.999
	One-class dominant	0.816	0.621	0.708	0.042	0.032	0.019	0.037	0.000	0.785	0.878	0.795	0.999
Citeseer	Equal proportion	0.251	0.334	0.147	0.000	0.003	0.003	0.001	0.000	0.950	0.943	0.980	0.999
	Random split	0.102	0.335	0.244	0.002	0.000	0.007	0.002	0.000	0.993	0.908	0.956	1.000
	One class missing	0.464	0.625	0.692	0.006	0.111	0.147	0.115	0.000	0.838	0.802	0.783	0.999
	Single class only	1.589	1.615	1.292	0.002	0.534	0.544	0.050	0.000	0.477	0.450	0.469	0.998
	One-class dominant	1.154	1.322	0.928	0.000	0.034	0.056	0.042	0.000	0.615	0.412	0.710	1.000
AC	Equal proportion	0.495	0.370	0.706	0.000	0.006	0.003	0.084	0.000	0.852	0.928	0.746	1.000
	Random split	0.082	0.708	0.953	0.007	0.000	0.012	0.016	0.000	0.995	0.709	0.564	0.999
	One class missing	0.282	0.788	0.665	0.002	0.054	0.086	0.027	0.000	0.950	0.695	0.810	0.999
	Single class only	1.818	1.537	1.874	0.012	0.378	0.470	0.387	0.002	0.227	0.583	0.189	0.999
	One-class dominant	1.075	1.155	1.544	0.001	0.022	0.036	0.063	0.000	0.715	0.609	0.166	1.000

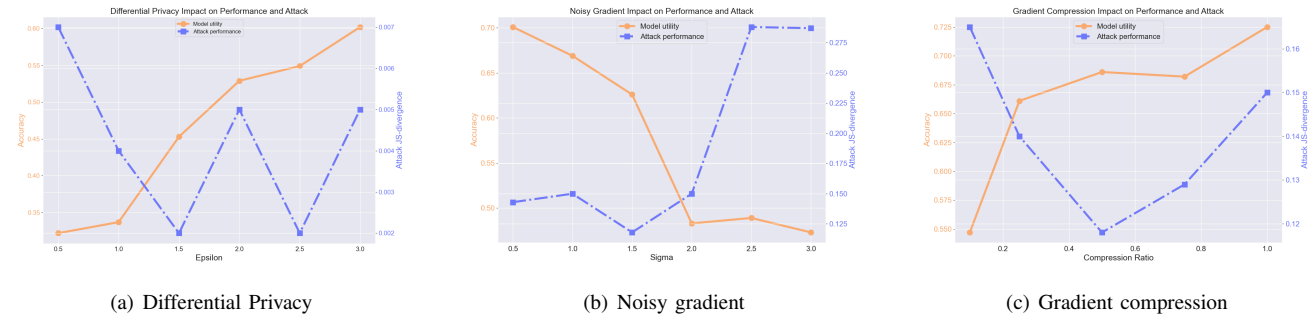


Fig. 2: Model utility (accuracy) and attack effectiveness (JS-divergence) under three defense strategies: (a) Gradient compression, (b) Noisy gradient, and (c) Differential privacy. For the plot, we measure the robustness when using GCN model and Cora dataset.

shared/common auxiliary samples across processes (our auxiliary sets are small, 20%). Across most partitions and datasets the number of shadow FL processes is positively correlated with attack performance; two exceptions are for Partition 2 on Amazon Computers (Figure 3(b)) and Partition 3 on Cora (Figure 3(c)) the best cosine similarity values were obtained at 14 and 16 FL processes, respectively.

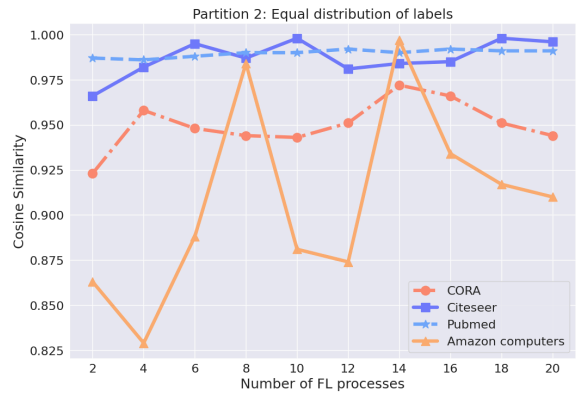
Partition 1 (shown in Figure 3(a)). In this partition, all the clients consist of a random class distribution. For the Cora and Amazon Computers dataset, CS reaches 0.99 when the number of FL processes is 20. In contrast, for the PubMed dataset, the attack achieves high CS with far fewer FL processes, likely because it is a much larger graph and the use of 20% of the data as the auxiliary set produced richer training examples. Based on the results of all the datasets, we use 20 shadow FL training processes to represent Partition 1.

Partition 2 (shown in Figure 3(b)). For this data partition,

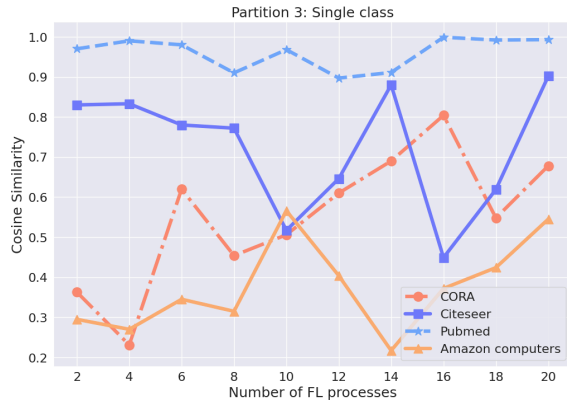
we first need to find the best number of clients that produces the best attack performance. Figure 4(a) reports the results on changing the number of clients having equal distribution labels within a single FL process, where the x -axis indicates the number of clients (e.g., $x=1$ means only one client has an equal distribution, and the rest have a random distribution). CS generally increases as the proportion of equal distribution clients grows. Amazon Computers shows the largest gain (from 0.84 up to 0.99), while Citeseer and PubMed remain relatively stable (Figure 4(a)). For each dataset, we first selected the optimal client proportion and then determined the required number of FL processes. For example, Amazon Computers performs best when all clients (10 clients) are uniform, so for Partition 2, in this dataset, we configured every FL process to have all clients uniformly distributed. Using this approach, we used 14 FL processes for Amazon Computers and for Cora (with 10 and 8 clients per process being equally



(a) Partition 1: Random distribution



(b) Partition 2: Equal proportion



(c) Partition 3: Single class



(d) Partition 4: Missing class

Fig. 3: Figure illustrating the impact of the attack when the number of shadow FL training is varied. Plots (a-d) show the relation of cosine similarity and the number of shadow FL training processes for Partition 1: Random distribution, Partition 2: Equal proportion, Partition 3: Single class, and Partition 4: Missing class. Note that all figures were plotted using GCN as a local model when training both the FL and shadow FL models.

distributed, respectively). For PubMed and Citeseer, we used 10 FL processes, with 5 and 6 clients per process set to equal distributions, respectively.

Partition 3 (shown in Figure 3(c)): We selected hyperparameters for Partition 3 with the same two-step procedure (choose the number of clients and then choose the number of FL processes). As shown in Figure 4(b), the Cora and Amazon Computers dataset displayed more fluctuations, whereas Citeseer decreases, and PubMed shows stability throughout the change of the number of clients. Therefore, we use 10 clients with the Partition 3 single class distribution for all datasets except Citeseer, where we use only 2 such clients. We observed a reduction in attack performance for Cora and Amazon when tuning the number of FL processes, which may be caused by the attack model used for hyperparameter selection was trained on data composed only of Partition 3. The final numbers of FL processes for Partition 3 are 10 FL processes for Amazon Computers, 14 for Cora, 16 for PubMed, and 20 for Citeseer.

Partition 4 (shown in Figure 3(d)): Figure 4(c) examines the “missing class” partition. Cora shows a noisy pattern but can reach high similarity (0.95) when only one client has a missing class. And Amazon Computers and Citeseer show similar behavior. In PubMed, we observe a clear improvement as the number of clients with missing classes increased (Figure 4(c)). In terms of the number of FL processes, Citeseer, PubMed, and Amazon Computers achieve high attack performance even at low numbers of FL processes. It is possibly because only a single class is missing, and that effect can be overshadowed by the distance-based metrics we use. Cora, however, tends to benefit from increasing the number of FL processes. Therefore, based on the comparison, we set the Partition 4 configurations as follows. For Cora, we use 20 FL processes with 9 clients missing a class; for PubMed, we use 20 FL processes with 6 clients missing a class; and for Amazon Computers and Citeseer, we use 20 FL processes with 2 and 10 clients missing a class, respectively.

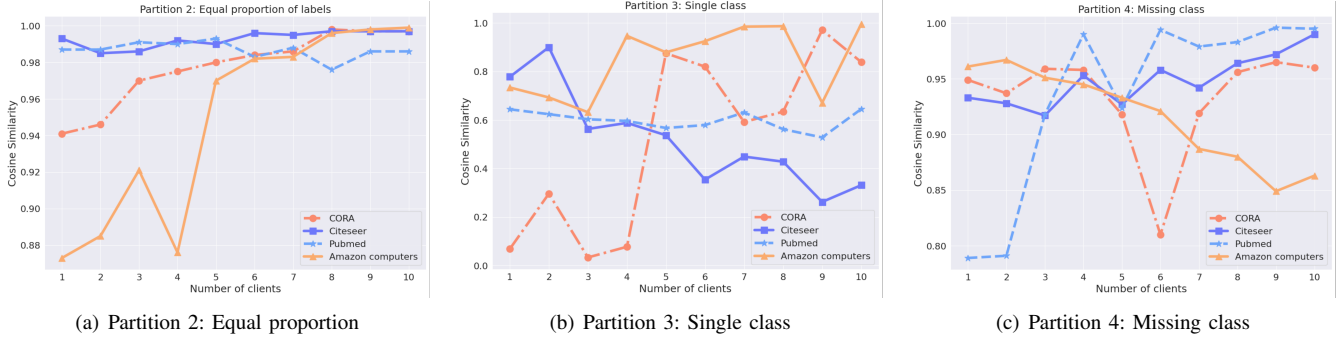


Fig. 4: This figure illustrates the impact of the attack when the proportion of clients with a specific Partition setting is changed. Subfigure a) shows the cosine similarity against the number of clients for Partition 2. Subfigure b) shows the cosine similarity against the number of clients for Partition 3. Subfigure c) shows the cosine similarity against the number of clients for Partition 4. Note that all figures were plotted using GCN as a local model in training both the FL and shadow FL models.

B. The Impact of Loss Function

TABLE V: Loss values and cosine similarity between the predicted and ground truth label distribution on various objective functions and their combinations. These values were obtained using an MLP-based attack model on the Cora dataset. MSE: Mean Squared Error, Var (L2): Distance of Variance (L2 norm), KL: Kullback-Leibler Divergence.

Objective function	Loss values (↓)	Cosine similarity (↑)
MSE	0.006	0.946
JS-div	0.132	0.995
Var (L2)	0.040	0.887
L1	0.047	0.981
KL	0.524	0.963
<i>Distribution + Alignment</i>		
JS-div + MSE	0.070	0.991
JS-div + Var (L2)	0.087	0.758
JS-div + L1	0.090	0.995
KL + MSE	0.267	0.994
KL + L1	0.289	0.797
KL + Var (L2)	0.282	0.807
<i>Alignment + Alignment</i>		
MSE + Var (L2)	0.025	0.934
L1 + MSE	0.027	0.994
L1 + Var (L2)	0.046	0.995
MSE + Var (L2) + L1	0.049	0.993
<i>Distribution + Distribution</i>		
KL + JS-div	0.330	0.820
<i>Distribution + Distribution + Alignment</i>		
KL + JS-div + MSE	0.338	0.889
KL + JS-div + L1	0.359	0.990
KL + JS-div + Var (L2)	0.357	0.985
<i>Distribution + Alignment + Alignment</i>		
JS-div + MSE + L1	0.095	0.905
JS-div + L1 + Var (L2)	0.112	0.990
JS-div + MSE + Var (L2)	0.091	0.989
KL + MSE + L1	0.296	0.980
KL + L1 + Var (L2)	0.312	0.903
KL + MSE + Var (L2)	0.291	0.807

Since the goal of our attack is to recover the true label distribution of the target client(s), we adopt objective functions specifically designed for distribution learning and evaluate on both individual and combined forms of alignment and distribution losses. For alignment loss, we select distance-

based measures such as L1 and Mean Squared Error (MSE), whereas for distribution learning, we employ divergence-based measures, including KL and JS-div. These choices are motivated by prior studies that have applied similar objectives in either label distribution inference attack or distribution learning tasks [31], [38], [39]. Through the combination of different alignment and distribution losses, we try to find the best combination of loss functions that delivers the best attack performance for our label inference distribution attack.

Table V illustrates the effects of various objective functions and their combinations on the attack performance, evaluated using loss values and cosine similarity. We grouped the results by the types of objectives: distribution-based, alignment-based, and their combinations. Among the individual losses, MSE achieves the lowest loss of 0.006, but with moderate cosine similarity (0.946). In contrast, despite a higher loss, JS-divergence yields the highest cosine similarity of 0.995. Combining distribution-based losses (e.g., KL) with alignment-based losses (e.g., L1) significantly improved performance. For instance, the combination of JS-divergence with L1 loss and KL with MSE both reach near-perfect CS of 0.995 and 0.994, respectively. This suggests complementary behavior between distributional and alignment objectives. Alignment-only combinations, that is, pairing L1 loss with either MSE or variance (L2), result in high cosine similarity (up to 0.995) but relatively low loss. In contrast, combining only distribution-based objectives performed the worst. The performance results varied when incorporating all three types: distribution, alignment, and variance. Additionally, combining three objective functions that include JS-div with MSE degraded the performance compared to their individual case or only two combined. Based on the combined results of both loss and cosine similarity, we finally chose the combination of JS-div, L1 loss, and variance (L2), as our loss function in Eq (6), for the following reasons: (i) JS-div is effective at comparing the distribution overlap, which consistently yielded high cosine similarity across our experiments. (ii) L1 loss provides robustness against outliers compared to MSE [40], and it yields high

cosine similarity in all combined cases. (iii) Variance-based L2 term can reduce the variance mismatch across clients, which is relevant in federated settings where data heterogeneity is high. This combination selection method is also adopted by a previous work [31] that achieves a successful attack in image datasets.

VII. CONCLUSION

In this work, we investigate the crucial privacy leakage problem in FedGNNs settings, termed as label distribution inference attack. Specifically, we introduced Fed-Listing, a novel passive label distribution inference attack against the horizontal federated graph learning. By training the shadow FL process on the honest-but-curious server with the last-layer gradients of clients, Fed-Listing demonstrates strong effectiveness in inferring client label distributions across a variety of benchmark graph datasets and GNN architectures. The experimental results show that Fed-Listing consistently outperforms baselines, particularly under challenging non-i.i.d. scenarios such as single-class and one-class-dominant distributions. Moreover, we further evaluated the robustness of Fed-Listing against three widely adopted defense strategies, where the study reveals the difficulty in mitigating Fed-Listing by existing methods, signifying the importance of designing privacy-preserving mechanisms that account for label distribution leakage. One limitation of this work is its reliance on an auxiliary dataset, and we have not evaluated scenarios where such data are unavailable. Therefore, exploring the use of synthetic or mixed-source auxiliary data to replace real auxiliary samples is an important future direction.

VIII. AI-GENERATED CONTENT ACKNOWLEDGMENT

None of the text, figures, and tables in the manuscript were filled in using the generative AI. However, for some parts of the code, AI was used for efficiency. We assure the codes generated using AI were verified and mentioned in comments in the GitHub repository.

REFERENCES

- [1] A. Awasthi, A. K. Garov, M. Sharma, and M. Sinha, “Gnn model based on node classification forecasting in social network,” in *2023 International Conference on Artificial Intelligence and Smart Communication (AISC)*. IEEE, 2023, pp. 1039–1043.
- [2] Z. Guo and H. Wang, “A deep graph neural network-based mechanism for social recommendations,” *IEEE Transactions on Industrial Informatics*, vol. 17, no. 4, pp. 2776–2783, 2020.
- [3] K. Sharma, Y.-C. Lee, S. Nambiar, A. Salian, S. Shah, S.-W. Kim, and S. Kumar, “A survey of graph neural networks for social recommender systems,” *ACM Computing Surveys*, vol. 56, no. 10, pp. 1–34, 2024.
- [4] Y. Wang, Z. Li, and A. Barati Farimani, “Graph neural networks for molecules,” in *Machine learning in molecular sciences*. Springer, 2023, pp. 21–66.
- [5] X.-M. Zhang, L. Liang, L. Liu, and M.-J. Tang, “Graph neural networks and their current applications in bioinformatics,” *Frontiers in genetics*, vol. 12, p. 690049, 2021.
- [6] W. Jiang, J. Luo, M. He, and W. Gu, “Graph neural network for traffic forecasting: The research progress,” *ISPRS International Journal of Geo-Information*, vol. 12, no. 3, p. 100, 2023.
- [7] A. Sharma, A. Sharma, P. Nikashina, V. Gavrilenco, A. Tselykh, A. Bozhenyuk, M. Masud, and H. Meshref, “A graph neural network (gnn)-based approach for real-time estimation of traffic speed in sustainable smart cities,” *Sustainability*, vol. 15, no. 15, p. 11893, 2023.
- [8] C. Gao, X. Wang, X. He, and Y. Li, “Graph neural networks for recommender system,” in *Proceedings of the fifteenth ACM international conference on web search and data mining*, 2022, pp. 1623–1625.
- [9] S. Wu, F. Sun, W. Zhang, X. Xie, and B. Cui, “Graph neural networks in recommender systems: a survey,” *ACM Computing Surveys*, vol. 55, no. 5, pp. 1–37, 2022.
- [10] R. Liu, P. Xing, Z. Deng, A. Li, C. Guan, and H. Yu, “Federated graph neural networks: Overview, techniques, and challenges,” *IEEE transactions on neural networks and learning systems*, 2024.
- [11] C. Shiranthika, P. Saeedi, and I. V. Bajić, “Decentralized learning in healthcare: a review of emerging techniques,” *IEEE Access*, vol. 11, pp. 54 188–54 209, 2023.
- [12] X. Zheng, Z. Wang, C. Chen, J. Qian, and Y. Yang, “Decentralized graph neural network for privacy-preserving recommendation,” in *Proceedings of the 32nd ACM International Conference on Information and Knowledge Management*, 2023, pp. 3494–3504.
- [13] J. Zhang and I. Tal, “A systematic review of contemporary applications of privacy-aware graph neural networks in smart cities,” in *Proceedings of the 19th International Conference on Availability, Reliability and Security*, 2024, pp. 1–10.
- [14] Z. Liu, L. Yang, Z. Fan, H. Peng, and P. S. Yu, “Federated social recommendation with graph neural network,” *ACM Transactions on Intelligent Systems and Technology (TIST)*, vol. 13, no. 4, pp. 1–24, 2022.
- [15] S. Ahmed, F. Jinchao, M. A. Manan, M. Yaqub, M. U. Ali, and A. Rameem, “Fedgraphmri-net: A federated graph neural network framework for robust mri reconstruction across non-iid data,” *Biomedical Signal Processing and Control*, vol. 102, p. 107360, 2025.
- [16] M. Y. Balik, A. Rekik, and I. Rekik, “Investigating the predictive reproducibility of federated graph neural networks using medical datasets,” in *International Workshop on PRedictive Intelligence In MEDicine*. Springer, 2022, pp. 160–171.
- [17] D. Manu, J. Yao, W. Liu, and X. Sun, “Graphganfed: A federated generative framework for graph-structured molecules towards efficient drug discovery,” *IEEE/ACM Transactions on Computational Biology and Bioinformatics*, vol. 21, no. 2, pp. 240–253, 2024.
- [18] J. Geiping, H. Bauermeister, H. Dröge, and M. Moeller, “Inverting gradients-how easy is it to break privacy in federated learning?” *Advances in neural information processing systems*, vol. 33, pp. 16 937–16 947, 2020.
- [19] H. Yang, M. Ge, D. Xue, K. Xiang, H. Li, and R. Lu, “Gradient leakage attacks in federated learning: Research frontiers, taxonomy and future directions,” *IEEE Network*, 2023.
- [20] I. E. Olatunji, W. Nejdl, and M. Khosla, “Membership inference attack on graph neural networks,” in *2021 Third IEEE International Conference on Trust, Privacy and Security in Intelligent Systems and Applications (TPS-ISA)*. IEEE, 2021, pp. 11–20.
- [21] L. Bai, H. Hu, Q. Ye, H. Li, L. Wang, and J. Xu, “Membership inference attacks and defenses in federated learning: A survey,” *ACM Computing Surveys*, vol. 57, no. 4, pp. 1–35, 2024.
- [22] J. Liu, B. Chen, B. Xue, M. Guo, and Y. Xu, “Piafgnn: Property inference attacks against federated graph neural networks,” *Computers, Materials & Continua*, vol. 82, no. 2, 2025.
- [23] M. Drencheva, I. Petrov, M. Baader, D. I. Dimitrov, and M. Vechev, “Grain: Exact graph reconstruction from gradients,” *arXiv preprint arXiv:2503.01838*, 2025.
- [24] L. Sun, Y. Dou, C. Yang, K. Zhang, J. Wang, P. S. Yu, L. He, and B. Li, “Adversarial attack and defense on graph data: A survey,” *IEEE Transactions on Knowledge and Data Engineering*, vol. 35, no. 8, pp. 7693–7711, 2022.
- [25] Z. Dai, Y. Gao, C. Zhou, A. Fu, Z. Zhang, M. Xue, Y. Zheng, and Y. Zhang, “Decaf: Data distribution decompose attack against federated learning,” *IEEE Transactions on Information Forensics and Security*, 2024.
- [26] A. Wainakh, F. Ventola, T. Müßig, J. Keim, C. G. Cordero, E. Zimmer, T. Grube, K. Kersting, and M. Mühlhäuser, “User label leakage from gradients in federated learning,” *arXiv preprint arXiv:2105.09369*, 2021.
- [27] L. Meng, Y. Bai, Y. Chen, Y. Hu, W. Xu, and H. Weng, “Devil in disguise: Breaching graph neural networks privacy through infiltration,” in *Proceedings of the 2023 ACM SIGSAC Conference on Computer and Communications Security*, 2023, pp. 1153–1167.
- [28] M. Arazzi, M. Conti, S. Koffas, M. Kreck, A. Nocera, S. Picek, and J. Xu, “Label inference attacks against node-level vertical federated gnns,” *arXiv preprint arXiv:2308.02465*, 2023.

- [29] C. Zhou, Y. Gao, A. Fu, K. Chen, Z. Dai, Z. Zhang, M. Xue, and Y. Zhang, “Ppa: Preference profiling attack against federated learning,” *arXiv preprint arXiv:2202.04856*, 2022.
- [30] Y. Liu, P. Jiang, and L. Zhu, “Preference profiling attacks against vertical federated learning over graph data,” in *IEEE INFOCOM 2025-IEEE Conference on Computer Communications*. IEEE, 2025, pp. 1–10.
- [31] Y. Gu and Y. Bai, “Ldia: Label distribution inference attack against federated learning in edge computing,” *Journal of Information Security and Applications*, vol. 74, p. 103475, 2023.
- [32] R. Ramakrishna and G. Dán, “Inferring class-label distribution in federated learning,” in *Proceedings of the 15th ACM Workshop on Artificial Intelligence and Security*, 2022, pp. 45–56.
- [33] T. Cheng, F. Jie, X. Ling, H. Li, and Z. Chen, “Ec-lda: Label distribution inference attack against federated graph learning with embedding compression,” *arXiv preprint arXiv:2505.15140*, 2025.
- [34] Z. Wu, S. Pan, F. Chen, G. Long, C. Zhang, and P. S. Yu, “A comprehensive survey on graph neural networks,” *IEEE transactions on neural networks and learning systems*, vol. 32, no. 1, pp. 4–24, 2020.
- [35] B. McMahan, E. Moore, D. Ramage, S. Hampson, and B. A. y Arcas, “Communication-efficient learning of deep networks from decentralized data,” in *Artificial intelligence and statistics*. PMLR, 2017, pp. 1273–1282.
- [36] Y. Zhao, M. Li, L. Lai, N. Suda, D. Civin, and V. Chandra, “Federated learning with non-iid data,” *arXiv preprint arXiv:1806.00582*, 2018.
- [37] Z. Wang, Z. Chang, J. Hu, X. Pang, J. Du, Y. Chen, and K. Ren, “Breaking secure aggregation: Label leakage from aggregated gradients in federated learning,” in *IEEE INFOCOM 2024-IEEE Conference on Computer Communications*. IEEE, 2024, pp. 151–160.
- [38] X. Geng, “Label distribution learning,” *IEEE Transactions on Knowledge and Data Engineering*, vol. 28, no. 7, pp. 1734–1748, 2016.
- [39] O. Elharrouss, Y. Mahmood, Y. Bechqito, M. A. Serhani, E. Badidi, J. Riffi, and H. Tairi, “Loss functions in deep learning: A comprehensive review,” *arXiv preprint arXiv:2504.04242*, 2025.
- [40] Q. Wang, Y. Ma, K. Zhao, and Y. Tian, “A comprehensive survey of loss functions in machine learning,” *Annals of Data Science*, vol. 9, no. 2, pp. 187–212, 2022.
- [41] P. Sen, G. Namata, M. Bilgic, L. Getoor, B. Galligher, and T. Eliassi-Rad, “Collective classification in network data,” *AI magazine*, vol. 29, no. 3, pp. 93–93, 2008.
- [42] O. Shchur, M. Mumme, A. Bojchevski, and S. Günnemann, “Pitfalls of graph neural network evaluation,” *arXiv preprint arXiv:1811.05868*, 2018.
- [43] T. N. Kipf and M. Welling, “Semi-supervised classification with graph convolutional networks,” *arXiv preprint arXiv:1609.02907*, 2016.
- [44] W. Hamilton, Z. Ying, and J. Leskovec, “Inductive representation learning on large graphs,” *Advances in neural information processing systems*, vol. 30, 2017.
- [45] K. Xu, W. Hu, J. Leskovec, and S. Jegelka, “How powerful are graph neural networks?” *arXiv preprint arXiv:1810.00826*, 2018.
- [46] C. Dwork, “Differential privacy,” in *International colloquium on automata, languages, and programming*. Springer, 2006, pp. 1–12.
- [47] M. Abadi, A. Chu, I. Goodfellow, H. B. McMahan, I. Mironov, K. Talwar, and L. Zhang, “Deep learning with differential privacy,” in *Proceedings of the 2016 ACM SIGSAC conference on computer and communications security*, 2016, pp. 308–318.
- [48] L. Zhu, Z. Liu, and S. Han, “Deep leakage from gradients,” *Advances in neural information processing systems*, vol. 32, 2019.
- [49] Y. Lin, S. Han, H. Mao, Y. Wang, and W. J. Dally, “Deep gradient compression: Reducing the communication bandwidth for distributed training,” *arXiv preprint arXiv:1712.01887*, 2017.